WIND TURBINE DESIGN

N.D. Fowkes*, A.D. Fitt†,
D.P. Mason‡ and F. Bruce§

Industry representative

Richard Naidoo
Durban University of Technology, Durban, Natal, South Africa

Abstract

The brief was to design a 50kW wind turbine for an eco-village in the KZN coastal region north of Durban with a rated wind speed of 13.5m/sec and where wind speeds vary from 3.5 m/sec to 18 m/sec. Of particular interest was the axis orientation (horizontal or vertical), the number size and shape of blades, and turbine height. Whilst detailed engineering design involves issues well beyond those that could be sensibly addressed by the study group, we did attempt to set down the aerodynamic design principles for such an undertaking. The available information indicates that close to the theoretically available power output $\frac{16}{27}(\frac{1}{2}\rho U_w^3)A$ (the Betz limit) can be realized using either two or three blades of standard design, where U_w the wind speed (assumed fixed here), ρ is the density of the air, and A the rotor area.

1 Introduction

The largest turbine in the world currently is the ENERCON E126 and is located at Emden, Germany. It produces 7+ MWatts of energy, it's height is 135m and the blades are of diameter 126m. The turbine of interest here is a much more moderate

*School of Mathematics and Statistics, University of Western Australia, Crawley, WA 6009, Australia *email: fowkes@maths.uwa.edu.au*

†School of Mathematics, University of Southampton, Southampton SO17 1BJ UK. *email: adf@maths.soton.ac.uk*

‡School of Computational and Applied Mathematics, University of the Witwatersrand, Private Bag 3, WITS 2050, Johannesburg, South Africa. *email: david.mason@wits.ac.za*

§African Institute for Mathematical Sciences, Muizenberg, South Africa. *email: faikah.bruce@gmail.com*

design and is classified as being of medium scale. The turbine is to be designed to service an eco-village of 200 households on the north coast of Durban and produce 50 kwatts. Such turbines have a typical rotor drum diameter of 12.5m.

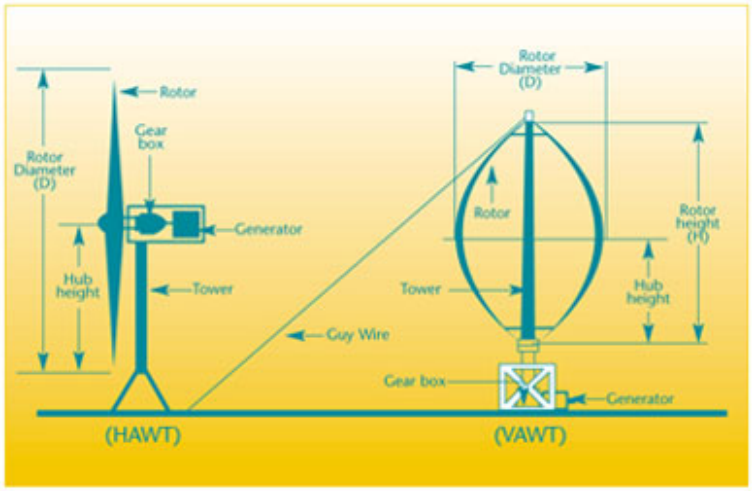

Figure 1: Turbine types

There are two types of wind turbines: vertical axis wind turbines (VAWT) often referred to as egg beaters because of their shape, and the conventional horizontal axis turbines (HAWT), see Figure 1. In general terms HAWTs are much more efficient (by a factor of about 7) than VAWTs in steady winds because they utilize lift forces as opposed to drag forces on the airfoils. However the HAWTs are omnidirectional and need to be continuously turned (using a passive vane or active mechanical/electrical controller) to face into the wind and are more expensive than VAWTs which are ground mounted. The VAWTs are thought to be more suitable under highly variable wind conditions. It was felt that steady sea breezes off Durban would make the HAWT design more suitable. In any case we worked on that assumption. After a brief description of the aerodynamic features of the turbine components, see Section 2, we will describe the known results in Section 3 and indicate how this knowledge may be used to design the turbine. Much of the work described here is based on results described in David Spera's (1994) excellent book 'Wind Turbine Technology', see especially Chapter 5.

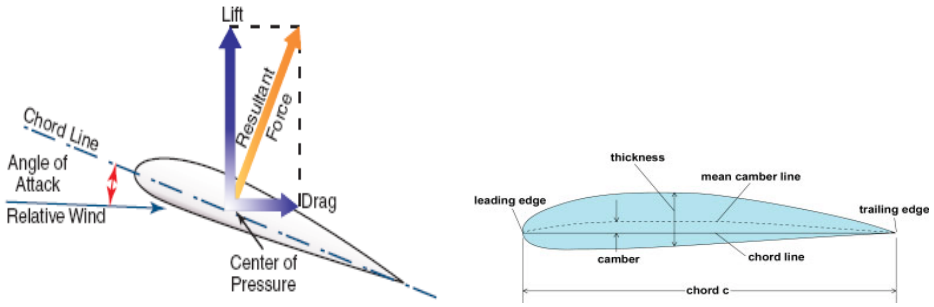

Figure 2: *Left:* Lift and drag forces on an airfoil. *Right:* Airfoil shape factors.

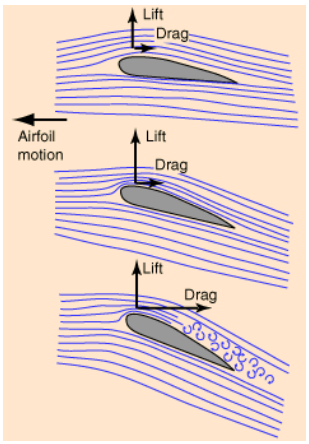

Figure 3: Stall: If the angle of attack exceeds α_{crit} the foil stalls.

2 Turbine Aerodynamic Components

The working core of the turbine are the blades which act as airfoils. In the presence of a wind, high lift forces (acting at right angles to the airfoil) are generated with little drag, providing the angle of attack α is less than a critical angle α_{crit} of about 10°. The angle of attack is the angle between the *relative* velocity of the wind to the cord direction which is very different to the wind direction in the turbine case because of the relatively high speed of rotation of the rotor, see Figure 2 Left; the tip speed ratio (defined to be the rotor tip speed divided by the wind speed) is typically 5 or 6. For angles of attack less than critical the lift force increases in proportion to the angle of attack. For angles of attack greater than critical, separation occurs at the leading edge of the airfoil so that the drag increases dramatically and the lift drops

to almost zero, a condition referred to as stall, see Figure 3. Stall may be avoided by choosing the pitch angle of the blades; variable pitch blades are sometimes used. The shape and roughness of the front edge of the airfoil dramatically effects the stall characteristics and the back edge needs to be sharp. Much work has been done on appropriately shaping the front edge especially but also designing the sectional shape to achieve required lift and drag characteristics especially in the aircraft industry, but also in the turbine context, see Spera (1994). Standard designs are available off the shelf.

The blades are tapered and twisted and the blade tips may be kinked. The reason for these design features is primarily aerodynamic but also mechanical. Vortices shed from the tip of the blades represent a significant loss of useful energy which can be reduced by shaping. (Tip loss factors can be applied to quantify the loss, see Spera p236.) Additionally less torque is required to set a tapered blade in motion.

Almost universally modern turbines have two or three blades; these being aerodynamically optimal, see later. The tip speed ratio is tuned so that the power output from the turbine is maximized in either case. Both are (almost) equally aerodynamically efficient (two bladed turbines capture about 5 % less energy) but two bladed turbines require higher tip speed ratios to yield the same energy output as three bladed turbines. This is a disadvantage both with regard to noise and visual intrusion. Furthermore two bladed turbines are subject to significant gyroscopic forces, require a hinged (teetering hub) rotor, and the higher shaft rotation speeds increase gearbox and transmission costs. Most modern turbines are three-bladed. Solidity has to be taken into account when deciding on the number of blades to use. Solidity is the ratio of the total blade area to the swept area. A low solidity results in higher speeds and low torque, whereas a high solidity results in lower speeds and higher torque.

To ensure the wind turbine is producing the maximal amount of electric energy at all times, a yaw drive is used to keep the rotor at right angles to the wind. Medium size turbines usually have an active yaw system; an anemometer on the nacelle tells the controller which way the wind is blowing. Increasingly sophisticated field wind detection systems are being employed to enable (larger) turbines to adjust to changing wind directions.

Blades made out of wood are inexpensive, strong and lightweight. Metal blades such as aluminium and steel blades are expensive and are subject to metal fatigue. Most turbine blades are constructed using fiberglass. Fiberglass is lightweight, strong, inexpensive and has good fatigue characteristics.

3 A Dimensional Analysis of the Problem

The maximum available power from the wind per unit area is

$$P_w = \frac{1}{2}\rho U_w^3 :$$

where U_w the velocity of the wind (assumed fixed here) and ρ is the density of the air. In order to extract this power one would need an energy extraction device that would reduce the wind's velocity to zero without changing the temperature. No such ideal device exists, however this expression provides us with appropriate standard for measuring the efficiency of real turbines. Explicitly if P_T is the power output of a turbine with rotor area A then the aerodynamic efficiency is defined to be

$$\mathcal{E}_T = \frac{P_T/A}{P_w} = \text{fn}(\lambda, \alpha, \text{dimensionless blade shape factors}, B, \text{Re}, \cdots); \qquad (3.1)$$

in the literature this is referred to as the rotor power coefficient (C_P). The efficiency as defined is dimensionless, and in the horizontal axis turbine of interest will depend on the choice of the various design parameters which are best expressed in dimensionless form. In (3.1) these dimensionless parameters are listed in order of importance. We have:

1. $\lambda = (\Omega D/2)/U_w$ is the tip speed ratio, where Ω is the angular velocity of the rotor and D is the rotor diam,
2. α is the pitch angle or angle of attack, see Figure 2 Left.
3. S is the 'solidity' defined to be the ratio of the projected area of blades to the rotor area$A$
4. B is the blade number
5. Dimensionless blade shape factors refer to length to width ratio, taper and twist angles, tip shape etc.
6. Dimensionless blade section shape factors refer to the various aerodynamically significant features of the blade section (blade thickness to chord ratio, leading edge shape factors etc.), see Figure 2 Right.
7. Other fluid dynamic parameters such as the Reynolds number (Re) of the flow.

A complete knowledge of the functional dependence expressed in (3.1) would enable one to immediately determine the performance of any turbine. Our understanding of the physics is not sufficiently complete to determine this function,

however a variety of theoretical and computational models have been developed to shed light on the important aspects of the problem and, when combined with experimental results, provide sufficient information to effectively determine $\mathcal{E}_T$.

Now for any tip speed ratio there is an optimal choice for α which we will denote by $\alpha_{opt}(\lambda)$. You will recall that the lift and drag forces on the airfoils vary strongly with α, and in particular α should be chosen to maximize lift while avoiding stall. If we assume this sensible choice is made then the functional dependence can be simplified to the form

$$\mathcal{E}_\mathcal{T} = \text{fn}(\lambda, S, B, Re, \cdots);$$

the actual function will of course differ from the earlier expression.

The Betz Limit

The major performance limitation to the HAWT is caused by *retardation*. The rotor (in operation) necessarily obstructs the flow. The air pressure immediately upstream of the rotor is higher than that downstream and surrounding the rotor, so that the air stream is partially diverted away from the rotor, as shown in Figure 4. This means that the flux of air through the rotor is somewhat less than one might anticipate, and the area ratio A_1/A_2 as seen in Figure 4 provides a measure for the associated reduced efficiency. In order to determine the area ratio A_1/A_2 and the associated efficiency one would need to solve for the flow around the particular turbine, however Rankine-Froude Theory (or actuator theory) shows that there exists an upper limit for this ratio given by the celebrated Betz Limit ($A_1/A_2 = 2/3$ with $\mathcal{E}_\mathcal{T} = 16/27$). The theory replaces the rotor by an 'actuator disc' that mimics the pressure drop without relating it to the rotor aerodynamic features. In spite of this limitation this is undoubtedly the most important theoretical result in turbine theory. Since there is no possibility of improvement beyond this limit it makes sense to accept the Betz limit as a new 'gold standard' and to rewrite,

$$\mathcal{E}_\mathcal{T} = \frac{16}{27}\text{fn}(\lambda, S, B, t/b, Re, \cdots) \tag{3.2}$$

where of course the upper bound on fn(.) is unity. Whilst we cannot do better than $\mathcal{E}_\mathcal{T} = \frac{16}{27} \approx 0.59$ it is a remarkable fact that one can get very close to the Betz limit and this fact greatly effects our approach to design.

An outline of the derivation of the Betz limit for the power coefficient is given in Appendix A.

Rotation in the Wake: λ, S, B, $\cdots$ effects

The rotor induces air rotation in it's wake. In fact the flow in the wake rotates in the opposite direction to the rotor because the wind turbine extracts energy from the

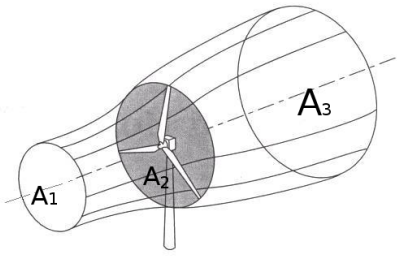

Figure 4: Retardation: The Betz limit

flow, see Spera (1994), and Manwell (2002). Any such rotation represents an energy loss from the system. The actual amount will depend on all the design parameters in a complicated way however, as one might expect, it is the tip speed ratio that is the primary determinant. A refinement of actuator disc theory taking into account rotor and wake rotation was first introduced by Joukowski (1918) and lead to Optimum Actuator Disk, or Glauert Theory (1935), which produces a still better estimate than the Betz limit of the upper efficiency of a rotor as a function of λ, see Figure 5. It should be noted that the Betz limit is realized at $\lambda \to \infty$ limit, although this limit cannot be practically realized. However note that for $\lambda \approx 5$ the efficiency realized is within 5% of the Betz limit. This theory again does not model individual blades (correctly) and so cannot be used for detailed design. In particular Glauert theory does not account for the circulation introduced around the individual airfoils (and thus the lift) and the vorticity shed from their trailing edges.

The choice for λ is a primary design feature since it greatly effects the energy extraction rate from the rotor. The rotor applies torque to a shaft connected by gears to a dynamo which generates electricity. In the zero torque case the rotor rotates rapidly (so λ is large) but there is no energy extraction; the rotor is simply spinning freely and churning up the air. Of course the energy extraction rate when $\lambda = 0$ is also zero, so one would expect there an optimal to be reached at some intermediate λ value, and this is seen in Figure 5 which plots the power efficiency for a variety of blade numbers B and a variety of drag to lift ratios (D/L). This ratio is generally less than 0.02 for well designed turbines so the $D/L = 0$ curves are most relevant. The theoretical underpinning for these results and studies on rotor aerodynamics is 'Blade–Element (or momentum, or Strip) Theory', which goes back to Froude in 1878; see Spera (1994) p233. Essentially the theory adds up the lift and drag forces acting on individual strips (treated as small sections of 2D airfoils) of blades at specified radial distances from the centre of the rotor, assuming no interaction between adjacent strips and more remote blades. This theory does

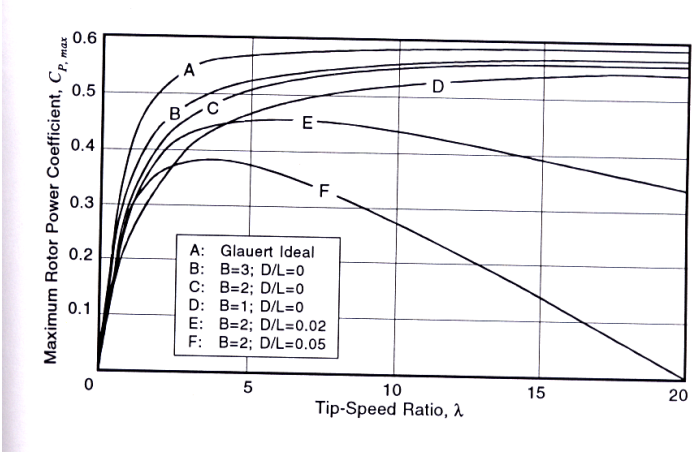

Figure 5: Glauert Theory and Blade Element Theory results: The effect of the tip speed ratio, the number of blades and the drag to lift ratio D/L on rotor performance.

produce explicit analytic results which approximately determine the effect of blade number and shape etc. on performance but various corrections have to be made to account for tip losses, the aerodynamic interaction between blades etc., so that in the end designers rely on empirical results based on strip theory analysis but with fitted coefficients. An empirical result often used is

$$C_F = \frac{16}{27}\left[\frac{\lambda B^{0.67}}{1.48 + (B^{0.67} - 0.04)\lambda + 0.0025\lambda^2} - (\frac{1.92\lambda^2 B}{1 + 2\lambda B})\frac{D}{L}\right], \qquad (3.3)$$

which is plotted in Figure 5, where the Betz limits and Glauert ideals are also plotted. Note especially that the efficiency results achieved by practical turbines are within 15%' of the Betz limit, which provides justification for the simple design strategy to be adopted, see later. Also note that the efficiency curves reach a peak (or at least flatten out) for values of $\lambda \approx 5$ for all blade numbers. Since higher speeds are mechanically less desirable, $\lambda \approx 5$ represents sensible design. The effect of blade number on aerodynamic performance is again seen to be marginal for B ranging from 1 to 3, however mechanical vibration issues favor turbines with 3 blades as mentioned earlier.

Recall that the solidity is the ratio of the plan form area of the blades to the rotor area and is typically less than 0.1 for modern wind turbines. A change in solidity changes many aerodynamic factors and the effects of solidity and blade number cannot be easily separated out, however typically the range $S = 0.03$ to 0.04 is used

for $B = 2$ and $S = 0.08$ to 0.09 for $B = 3$, and, providing one remains within this range, the efficiency level seems to be relatively unaffected.

Computationally intensive 3D steady models based on vortex theory have been developed, see Gohard (1978). Such sledge hammer approaches attempt to model the aerodynamic interaction between the individual blades and with the global environment, but are perhaps heavy handed for turbine design. Such studies may be useful for blade design.

4 A Simple Design Procedure

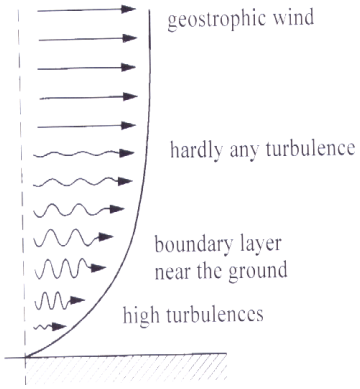

Figure 6: A typical wind profile

Based on the above observations it makes sense to use the Betz limit, see (3.2) for first order design, which indicates that the power output for a turbine is expected to be given by

$$P_T = A\frac{16}{27}(\frac{1}{2}\rho U_w^2), \quad A = \pi(D/2)^2, \tag{4.1}$$

see (3.1), where D is the rotor diameter. An additional 20% design margin would be prudent, to take into account the aerodynamic inefficiencies as seen in Figure 5. Also electrical/mechanical inefficiencies should be correctly accounted for.

Note especially that the power output varies in proportion to $U_w^3 D^2$, and so is very sensitive to (assumed steady) wind speed. This is of course why wind turbines are placed on high towers and if possible on the top of hills and on cleared regions. As a rule of thumb the wind speed increases by approximately 20% for every additional 10m height H due to wind shear in the ground boundary layer, which corresponds

to a 34% increase in power output; very significant! Power law (or log layer) models of the form

$$U_w(z) = U_R(z/z_R)^\alpha$$

are normally used to describe the wind profile, where U_R is the wind speed at a reference elevation z_R, and α needs to be fitted to local data and depends on tree cover etc., see Figure 6; a boundary layer thickness of 15m is typical.

Evidently for a given power output (50kwatts in our case) $U_w^3(H)D^2$ is fixed so that the choice needs to be between a larger rotor diameter turbine based on a small tower or a smaller diameter rotor on a tall tower. The choice needs to be based on the associated cost function $C(H, D)$; where both building and ongoing costs need to be assessed. As indicated earlier the other design features have a marginal effect on performance but evidently should be based on best practice (eg $B = 2$ or 3 with $S = 0.03,$ or 0.07 etc.) with associated costs in mind.

Another major design and siting consideration is wind variability both over a day and annually, see Chapter 8 in Spera (1994). A variety of empirical models have been developed to describe the local wind speed variability in a useful way so that an assessment can be made of the turbine performance over a year, the most popular of which is the Weibull model, see Spera (1994). Such models fit parameters using statistical data collected locally. Evidently dependability, energy storage and capacity credit issues arise and the design of hybrid systems depends on such information.

In conclusion we re-iterate that the aerodynamic design issues addressed here are but a small part of the overall design problem and that our understanding in this area is very good. It goes without saying that a detailed understanding of the local wind conditions is absolutely necessary if success is to be assured.

References

Spera, D.A. (1994). *Wind Turbine Technology,* ASME Press, New York.

Gohard, J.D. (1978). *Free Wake Analysis of Wind Turbine Aerodynamics. TR 184-14*, Massachusetts Inst. of Technology. Cambridge, Mass.

Joukowski, N.E. (1918). *Travaux du Bureau des Calculs et Essais Aeronautiques de l'Ecole Superieure Technique de Moscou.*

Glauert, H. (1976). *Airplane Propellers. Aerodynamic Theory,* (ed W. F. Dyrand), Div L. Chapter XI, Springer Verlag, Berlin. (Reprinted by Peter Smith, Gloucester, MA 1976).

Manwell, J.F., Gowan, J.G. and Rogers, A.L. (2002). *Wind Energy Explained: Theory, Design and Applications.* J Wiley and Sons, Ch 3.

Betz, A. (1926). *Windenergie und Ihre Ausnutzung dirch Wendmullen.* Vandenhoek und Ruperecht, Gottingen, Germany.

Appendix A.1: The Betz Limit

The Betz limit is derived using the actuator disk model which is based on linear momentum theory. The rotor is modelled as a uniform disk (Spera 1994, Manwell *. et al.* 2002).

The derivation uses a control volume which is bounded by the surface of the stream tube and the downstream and upstream cross-sections of the stream tube as shown in Figure A.1. The only flow of air is across the ends A_1 and A_4 of the stream

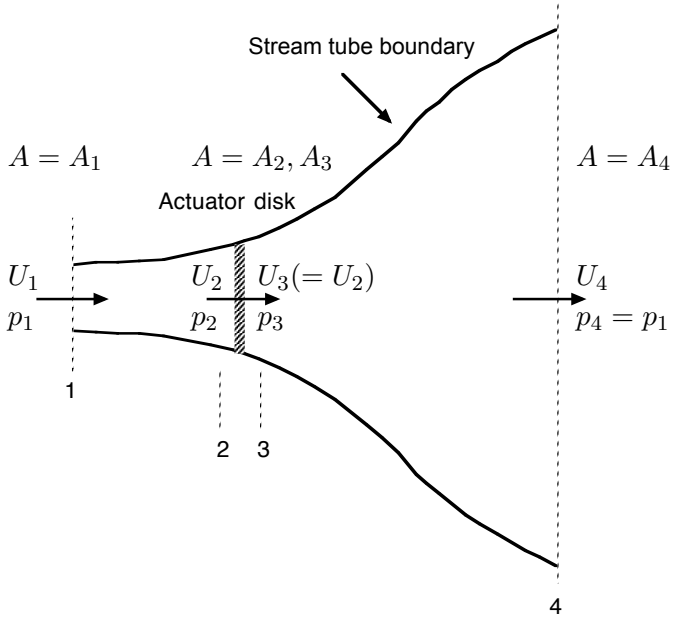

Figure A.1: Actuator disk model showing regions $(1, 2, 3)$ in the stream tube, adapted from J.F. Manwell et al. (2002). In the Betz limit (with maximum power coefficient C_P) the working conditions are $A_1 = \frac{2}{3} A_2, A_4 = 2A_2$, with $U_2 = U_3 = \frac{2}{3} U_1$ and $U_4 = \frac{1}{3} U_1$, and with $p_2 = p_1 + \frac{5}{18} \rho U_1^2$ and $p_3 = p_1 - \frac{1}{6} \rho U_1^2$.

tube. The actuator disk of area A_2 creates a discontinuity in the pressure, $p_3 - p_2$, in the stream tube of air flowing through it.

It is assumed that the fluid is incompressible, that the flow is steady and that there is no rotation in the wake. The pressure far upstream of the rotor, p_1, and far downstream of the rotor, p_4, are assumed to be equal to the undisturbed static pressure and therefore $p_4 = p_1$. It is also assumed that the force of the wind on the disk is uniform and that the velocity across the disk remains the same so that $U_3 = U_2$.

Since the flow is steady and there is no flow of mass through the curved boundary of the stream tube, the rate of flow of mass across the cross-sections A_1, A_2 and A_4 is conserved. Hence

$$\rho\, A_1\, U_1 = \rho\, A_2\, U_2 = \rho\, A_4\, U_4 \ . \tag{A.1}$$

Denote by T the thrust force of the wind on the disk. Then

$$T = A_2(p_2 - p_3) \ . \tag{A.2}$$

But the net force on the total volume enclosing the whole of the stream tube bounded by A_1 and A_2 is equal and opposite to T. Applying conservation of linear momentum to this control volume gives

$$-T = (\rho\, A_4\, U_4)U_4 - (\rho\, A_1\, U_1)U_1 \ , \tag{A.3}$$

which may be rewritten, with the aid of (A.1), as

$$T = \rho\, A_2\, U_2(U_1 - U_4) \ . \tag{A.4}$$

Since $T > 0$, it follows that $U_4 < U_1$.

Now, no work is done on the upstream or downstream side of the rotor. Thus Bernoulli's theorem can be applied to the stream tube on either side of the disk:

$$\text{upstream} \qquad p_1 + \frac{1}{2}\,\rho\, U_1^2 = p_2 + \frac{1}{2}\,\rho\, U_2^2 \ , \tag{A.5}$$

$$\text{downstream} \qquad p_3 + \frac{1}{2}\,\rho\, U_3^2 = p_4 + \frac{1}{2}\,\rho\, U_4^2 \ . \tag{A.6}$$

But we have assumed that $p_4 = p_1$ and that there is no velocity change across the disk so that $U_2 = U_3$. Thus (A.6) becomes

$$p_3 + \frac{1}{2}\,\rho\, U_2^2 = p_1 + \frac{1}{2}\,\rho\, U_4^2 \ . \tag{A.7}$$

Equations (A.2), (A.4), (A.5) and (A.7) form the basis of the derivation.

We first rewrite (A.2) for T. From (A.5) and (A.7),

$$p_2 - p_3 = \frac{1}{2}\,\rho(U_1^2 - U_4^2) \tag{A.8}$$

and therefore (A.2) becomes

$$T = \frac{1}{2}\,\rho\, A_2(U_1^2 - U_4^2)\ . \tag{A.9))}$$

Equation (A.4) and (A.9) gives

$$U_2 = \frac{1}{2}\,(U_1 + U_4)\ . \tag{A.10}$$

Thus the wind speed at the actuator disk is the average of the upstream and downstream wind speeds.

The axial induction factor, a, is defined as

$$a = \frac{U_1 - U_2}{U_1}\ . \tag{A.11}$$

It is the fractional decrease in the wind speed between the downstream free stream and the plane of the disk. We can now express U_2 and U_4 in terms of a and U_1 using (A.10) and (A.11):

$$U_2 = (1-a)\,U_1\ , \tag{A.12}$$

$$U_4 = (1-2a)\,U_1\ , \tag{A.13}$$

The axial induction factor is a measure of the affect of the turbine on the wind. As a increases from zero, the wind speed in the far wake, U_4, steadily decreases. The minimum value of U_4 is zero and therefore the maximum value of a is 0.5. The model is not valid for $a > 0.5$.

The power output, P, is the rate of working of the thrust T and is the product of T and the wind velocity at the disk, U_2:

$$P = T\,U_2 = \frac{1}{2}\,\rho\, U_!^3\, A_2\, 4a(1-a)^2\ . \tag{A.14}$$

The power coefficient, C_P, is defined by

$$C_P = \frac{\text{rotor power}}{\text{power in the wind}} = \frac{P}{\frac{1}{2}\,\rho\, U_1^2\, A_2} \tag{A.15}$$

and therefore

$$C_P = 4a(1-a)^2\ . \tag{A.16}$$

The maximum value $C_P(a)$ occurs at $a = \frac{1}{3}$ and takes the value

$$C_{P,\max} = \frac{16}{27} = 0.598 \; . \tag{A.17}$$

Equation (A.17) is the Betz limit. It is the maximum theoretical value for the power coefficient C_P.

When $a = \frac{1}{3}$, it follows from (A.12) and (A.13) that

$$U_2 = \frac{2}{3} U_1 \; , \qquad U_4 = \frac{1}{3} U_1 \tag{A.18}$$

and from (A.1), (A.5) and (A.7) that

$$A_1 = \frac{U_2}{U_1} \, A_2 = \frac{2}{3} \, A_2 \; , \qquad A_4 = \frac{U_2}{U_4} \, A_2 = 2A_2 \; , \tag{A.19}$$

$$p_2 = p_1 + \frac{5}{18} \, \rho \, U_1^2 \; , \qquad p_3 = p_1 - \frac{1}{6} \, \rho \, U_1^2 \; . \tag{A.20}$$

When the power coefficient has a maximum value the stream tube for flow through the disk has an upstream cross-sectional area of $\frac{2}{3}$ the disk area and its cross-sectional area grows to twice the disk area in the downstream wake. The pressure drop across the disk is

$$p_2 - p_3 = \frac{4}{9} \, \rho \, U_1^2 \; . \tag{A.21}$$

The model is not valid for axial induction factors, a, greater than 0.5. The dependence of the physical parameters on a is illustrated in Figure A.2. The pressure p_3 on the downstream side of the disk takes its minimum value when $a = \frac{1}{3}$. This is the value of a for which C_P attains its maximum value.

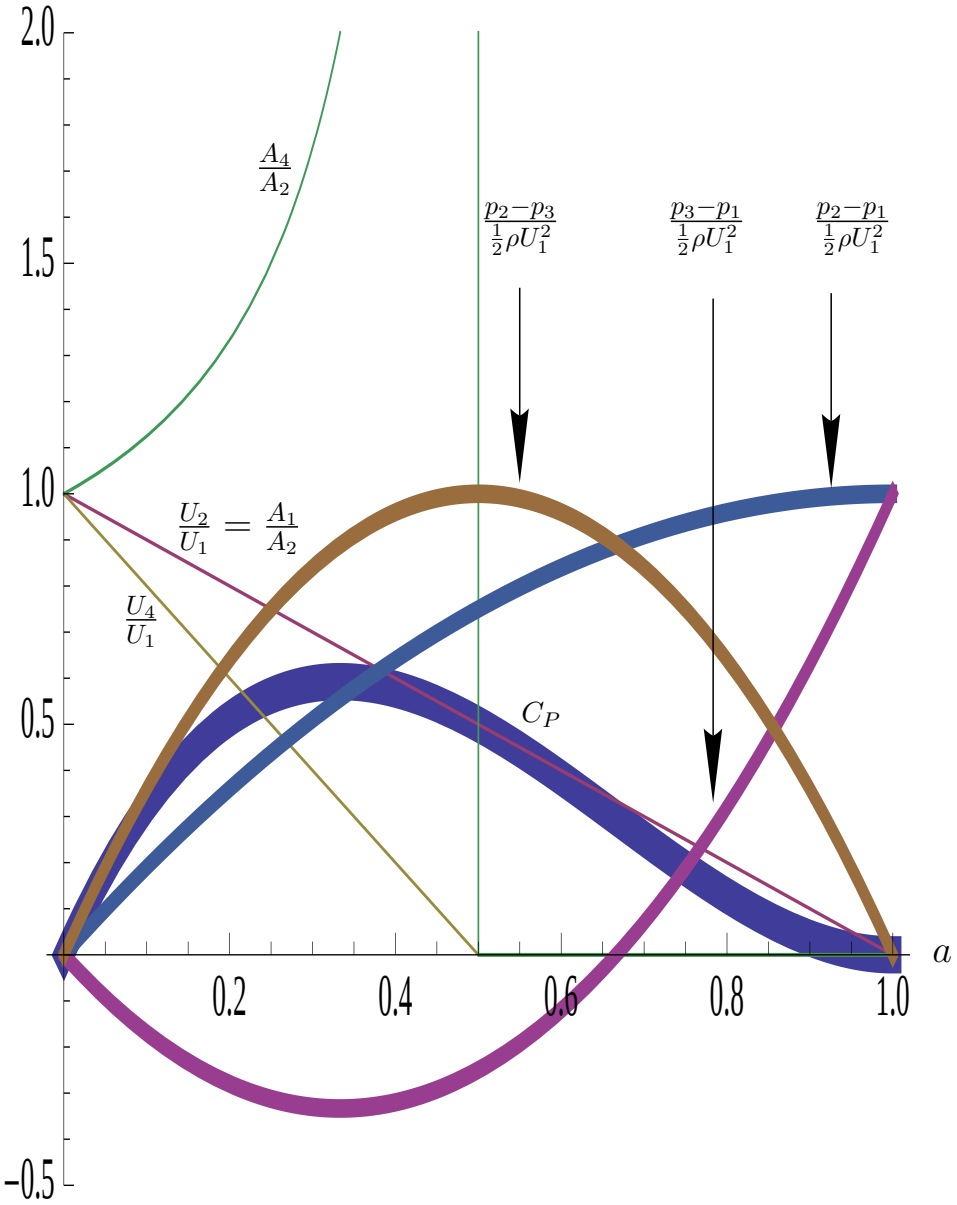

Figure A.2: Physical parameters in the Betz model. The pressures (medium thickness curves) and velocities (thin curves) are presented at the three locations $(1, 2, 3)$ (see Figure A.1) as a function of the induction factor a. The power coefficient C_P (thick curve) is also plotted. The Betz model is not valid for $a > 0.5$.